STM JOURNALS

Journal of
Polymer & Composites

ISSN: 2321-2810 (Online)
ISSN: 2321-8525 (Print)
Volume 14, Special Issue 3, 2026
DOI (Journal): 10.37591/JoPC

https://journals.stmjournals.com/jopc

Research JoPC

Catalytic Performance Improvement in Polymer Derived Nanostructures for Fuel Cell Applications

Prasad M. Patare[1], Ganesh P. Dawange[2], P. William[3,*], Dharmendra Kumar Roy[4], Pravin B. Khatkale[5]

Abstract

The performance and operational lifetime of PEMFCs are closely linked to the catalytic activity and durability of cathode electrocatalysts. In this research, a polymer-derived cobalt–iron nitrogen-doped carbon (CoFe–N/C) nanostructured catalyst is developed to enhance the ORR performance for PEMFC applications. PAN and melamine serve as nitrogen-rich polymer precursors, while cobalt and iron salts generate highly dispersed metal–nitrogen active sites within a porous carbon matrix through thermal treatment at 900 °C. The synthesized catalyst exhibits a high specific surface area of 612 $m^2 g^{-1}$ with abundant Co-N and Fe-N coordination sites, facilitating efficient electron transfer and oxygen adsorption. Structural characterization using XRD, Raman spectroscopy, SEM, TEM, and XPS confirms the successful formation of uniformly distributed nanostructures with enhanced graphitic properties. The PEMFC Performance Evaluation produced the best overall result because it directly validates the practical fuel cell performance of the synthesized CoFe–N/C catalyst. The catalyst achieved a peak power density of 0.82 W cm^{-2}, maximum current density of 1.58 A cm^{-2}, and open circuit voltage of 0.96 V, confirming excellent oxygen reduction activity, efficient electron transfer, and high electrochemical stability for advanced PEMFC applications. DFT calculations further confirm that the synergistic interaction among cobalt, iron, and nitrogen-coordinated carbon sites effectively reduces the reaction energy barrier and enhances catalyst durability for advanced PEMFC applications.

***Author for Correspondence**
P. William

[1]Associate Professor, Department of Mechanical Engineering, Sanjivani College of Engineering, Kopargaon, Maharashtra, India
[2]Assistant Professor, Department of Structural Engineering, Sanjivani College of Engineering, Kopargaon, Maharashtra, India
[2]Research Scholar, Department of Chemistry, Haribhai V. Desai College of Arts, Science and Commerce (Autonomous), Pune, Maharashtra, India
[3]Professor (Research), School of Computer Science and Technology, Karunya Institute of Technology and Sciences, Coimbatore, Tamil Nadu, India,
[3]Research Fellow, Centre for Research and Consultancy, UNITAR International University, Selangor, Malaysia
[4]Associate Professor, Department of Computer Science & Engineering, Hyderabad Institute of Technology and Management, Medchal, Hyderabad, Telangana, India
[5]Controller of Examination, School of Engineering and Technology, Sanjivani University, Kopargaon, Maharashtra, India

Received Date: May 22, 2026
Accepted Date: June 10, 2026
Published Date: June 20, 2026

Citation: Prasad M. Patare, Ganesh P. Dawange, P. William, Dharmendra Kumar Roy, Pravin B. Khatkale. Catalytic Performance Improvement in Polymer Derived Nanostructures for Fuel Cell Applications. Journal of Polymer & Composites. 2026; 14(Special Issue 3): S968–S979p.

Keywords: PEMFCs, polymer-derived nanostructures, oxygen reduction reaction (ORR), CoFe–N/C electrocatalyst

INTRODUCTION

Polymer-derived nanostructures have attracted considerable attention for the development of functional materials in PEMFC applications, owing to their properties such as catalytic activity, high surface area, controllable porosity, and increased electrical conductivity [1]. Polymer-derived nanostructures are usually fabricated via the controlled pyrolysis process of polymer precursors, allowing the fabrication of M-N-C type catalysts with nanostructured forms [2]. The potential application of these materials within the PEMFC systems includes acting as electrocatalysts for the ORR reactions at the cathode. When compared to platinum-based catalysts, polymer-derived catalysts are inexpensive and highly adaptable for use in fuel cells [3].Their porous morphology also facilitates rapid electron transfer and reactant diffusion, to enhance fuel cell performance.

The use of polymer-derived nanostructured catalysts has gained significant attention in automotive, portable electronic, and renewable energy storage applications due to their ability to reduce dependence on expensive noble metals. Catalysts act as effective means for improving the efficiency of fuel cells, their longevity, and reaction rate of electrochemistry in PEMFC system. Moreover, the use of transition metals including cobalt, iron, and nickel in nitrogen-doped carbon matrix contributes to improving catalysis and oxygen adsorption [4]. Although the above catalysts present significant benefits, there are some problems hindering their application in PEMFC system. These problems include poor durability, loss of performance due to catalyst degradation under acidic environment, corrosion of carbon, and less catalytic activity than commercial platinum catalyst [5].Although polymer-derived nanostructures provide assistances such as low manufacturing cost, high thermal, and customizable composition, it also exhibits disadvantages including complex synthesis procedures, possible metal leaching, and limited stability during prolonged fuel cell operation [6]. Additionally, ensuring that catalytic efficiency remains constant at different temperatures and humidity levels is equally important. Thus, research continues to be conducted towards designing high-performance polymer-based nano-catalysts with greater resistance, superior ORR reaction rates, and optimal structures for maximum efficiency and sustainability in PEMFC technology [7–8].

The conventional PEMFC electrocatalysts possess high cost, low durability, and deficient ability for oxygen reduction, making it difficult to manufacture fuel cells. Thus, there is an urgent need for novel and improved polymer-based nanocatalysts. To address these challenges, this research develops polymer-derived $CoFe-N/C$ nanostructured catalysts enhancing oxygen reduction activity, durability, and overall PEMFCs electrochemical performance efficiently. This catalyst provides an opportunity for developing highly durable and economical PEMFC systems.

Research Organization

Introduction to Section 1 highlights the significance of polymer-based CoFe-N/C nanostructured catalysts for PEMFC applications and states the aim of the research. Introduction to Section 2 summarizes the latest relevant literature review and determines the current research gap in PEMFC electrocatalysts. Materials, methods of preparation, characterization, PEMFC performance evaluation, and theoretical studies on DFT analysis are described in Section 3. The findings of the experiment and their discussions are presented in Section 4. Limitations of this research are highlighted in Section 5, and conclusions drawn in Section 6.

Related Work

Recent research enhanced the catalytic efficiency, stability, conductivity, and pollutant degradation capacity of PEMFC through nanomaterials, biochar composites, nanoMOFs, and hydrothermal synthesis. Table 1 shows the recent catalytic materials and methods.

Research Gap

Existing PEMFC catalysts rely heavily on noble metals or show limited durability and scalability. Non-precious metal catalysts often suffer from low stability, poor conductivity, or incomplete ORR efficiency. Many synthesis routes are complex, expensive, and difficult to control for achieving uniform active-site formation. Limited integration of high-surface-area polymer-derived CoFe–N/C nanostructures with strong ORR–PEMFC validation reported in previous studies [9–16]. In this research, a scalable polymer-derived CoFe–N/C catalyst with high surface area, strong metal–nitrogen active sites, improved conductivity, excellent ORR activity, and enhanced stability validated through PEMFC and DFT analysis.

MATERIALS AND METHODS

For this research, the integrated method of catalysts preparation, structure designing, thermal processing, structural analysis, fuel cell performance tests, and DFT calculations was developed to provide a complete model for creating novel polymer-derived CoFe–N/C electrocatalysts with improved oxygen reduction reaction activity.

Table 1. Literature survey of PEMFC catalytic methods.

Ref.	Objective	Method Name	Result with Values	Limitations
[9]	Enhanced ORR catalytic activity and durability in PEMFC systems.	Pt–Pd/SZ-GNP Catalyst	Higher mass activity and better electrochemical stability than conventional catalysts.	Expensive noble metals and difficult large-scale synthesis.
[10]	Improved electrocatalytic efficiency of Fe-NC catalysts for PEMFC applications.	Bromide-Ion-Boosted Fe–NC Electrocatalyst	High ORR activity with enhanced stability and electron transfer performance.	Long-term operational durability requires further research.
[11]	Developed conductive carbon-free ORR catalyst nanoparticles for hydrogen fuel cells.	Ozone-Assisted Hydrothermal Sb-SnO_2 Synthesis	Improved conductivity and corrosion resistance with enhanced ORR performance.	Lower conductivity compared with carbon-supported catalysts.
[12]	Optimized ionomer interaction in PEMFC electrodes for better efficiency.	Operando X-Ray Absorption Spectroscopy Analysis	Improved electrode utilization and fuel cell reaction efficiency.	Expensive and complex analytical setup.
[13]	Strengthened cobalt nanoparticle support interaction for catalytic enhancement.	Schiff Base Functionalized Cellulose-Co Nanoparticles	Better catalytic activity and nanoparticle dispersion stability achieved.	Limited thermal and electrochemical stability analysis.
[14]	Controlled nanoMOF structure for improved catalytic pollutant degradation.	Modulator-Controlled Co-Based NanoMOFs	Enhanced color degradation catalytic efficiency in aqueous media.	Limited validation for fuel cell applications.
[15]	Improved catalytic properties of $MnCo_2O_4$ using biopolymer-assisted synthesis.	Biopolymer-Assisted Hydrothermal $MnCo_2O_4$ Synthesis	Higher surface area and improved catalytic activity observed.	Industrial scalability and durability not fully validated.
[16]	Enhanced adsorption and catalytic removal of antibiotics using biochar composites.	CuO/Cu_2O/Cu/N-Codoped Biochar Synthesis	High antibiotic removal efficiency through adsorption and photo-Fenton catalysis.	Primarily focused on wastewater treatment applications.

Materials

PAN, average molecular weight ≈ 150,000), melamine ($C_3H_6N_6$), cobalt nitrate hexahydrate ($Co(NO_3)_2 \cdot 6H_2O$), iron nitrate nonahydrate ($Fe(NO_3)_3 \cdot 9H_2O$), N, N-dimethylformamide (DMF), Nafion solution (5 wt%), ethanol, and isopropanol were utilized for catalyst synthesis. Commercial carbon paper and Nafion 212 membrane were employed for PEMFC testing. All chemicals used in this research were of analytical grade and utilized without additional purification. Deionized water with a resistivity of 18.2 MΩ cm was consistently employed throughout all experimental procedures.

Figure 1 depicts the preparation of CoFe-N/C catalyst through the pyrolysis process using polyacrylonitrile and melamine as precursors along with the addition of cobalt and iron salts to create porous carbon with catalytic Co-N/Fe-N active sites.

Synthesis of Polymer-Derived $CoFe-N/C$ Nanostructures

The Polymer-derived $CoFe-N/C$ nanostructured were prepared through precursor mixing, stabilization, carbonization, acid etching, and secondary heat treatment. The method produced a porous carbon structure containing $Co-N$ and $Fe-N$ sites which acted as efficient catalysts during the oxidation process.

- *Preparation of polymer precursor solution:* PAN was dissolved in N, N-DMF at high temperatures using continuous stirring to form an even solution of the polymer. Melamine, which is rich in nitrogen, was used, followed by the addition of cobalt and iron nitrates as sources of

the metals. The mixture was continuously stirred to ensure uniform ion distribution and effective coordination with nitrogen atoms.

- *Drying and stabilization process:* The above-prepared suspension of the precursor was dried in a vacuum oven 90 °C for 12 h to completely remove residual solvent and obtain a solid composite material. Stabilization through oxidation took place under heating conditions to encourage PAN chain cyclization, increase thermal stability, and prepare for carbonization.
- *Carbonization and formation of active sites:* High temperature carbonization under a nitrogen atmosphere at 900 °C for 3 h using a tubular furnace with a heating rate of 10 °C min^{-1}. The polymer matrix during pyrolysis was changed into a conductive graphitic carbon material, while the interaction between cobalt and iron with nitrogen resulted in the development of evenly distributed Co-N and Fe-N coordination centers within the carbon network.
- *Acid leaching and secondary heat treatment:* After obtaining the carbonized product, it was treated with 0.5 M H_2SO_4 solution at 80 °C for 6 hours in order to eliminate any metallic components as well as other impurities that were still present. The material was further washed with deionized water until it had a neutral pH value (≈7) and dried at 80 °C for 10 hours. The next step was a second thermal treatment in nitrogen at 850 °C for 2 hours.

Structural and Morphological Characterization

The structural and morphological characterizations were done using some analysis to determine the crystallinity, graphitization degree, surface morphology, chemical composition, porosity, and active site distribution.

- *XRD:* XRD analysis was done on the structural properties of the synthesized catalysts using Cu-Kα radiation ($\lambda = 1.5406$ Å). The diffraction spectrum was done on the range of 2θ from 10° to 80° at the rate of scanning of 5°/min. This spectrum was further analyzed for studies related to the formation of graphite carbon and metals.
- *Raman spectroscopy:* Raman spectral analysis was performed on the sample using a 532 nm laser light source. The D/G band intensity ratio (I_D/I_G) was obtained to quantify the level of graphitization and the extent of structural defects in the carbon lattice.
- *SEM:* SEM analysis was conducted to evaluate the surface morphology, porosity, and particle distribution of the catalyst. High magnification allowed for the assessment of the nanostructure uniformity and pores developed after heat treatment.
- *TEM:* It was conducted to assess the nanostructure of the interior along with the dispersion of cobalt and iron species. The lattice planes and particle size distribution were assessed to confirm the development of the nanoscale active regions inside the carbon matrix.
- *XPS:* It performed to assess elemental compositions and chemical bonding. The high-resolution XPS spectra for $C\ 1s, N\ 1s, Co\ 2p$, and $Fe\ 2p$ were analyzed to elucidate the formation of active $pyridinic - N, graphitic - N, Co - N, and\ Fe - N$.

PEMFC Performance Evaluation

PEMFC performance was tested by the research of the membrane electrode assemblage, coating of catalyst, hot pressing, fuel cell test by means of humidified hydrogen-oxygen mixture and polarization curve evaluation.

- *MEA fabrication:* Catalyst-coated cathode electrode was fabricated using catalyst ink sprayed on carbon paper at a loading of 2 mg cm^{-2}. Platinum coated carbon paper was used as the anode. The cathode and anode were then heated at 130 °C under 1 MPa pressure for 3 minutes to bond them with a Nafion 212 membrane. Testing of the PEMFC was carried out using humidified hydrogen and oxygen gases, where the temperature was maintained at 80 °C, along with relative humidity control, ensuring reliable electrochemical efficiency and proton conductivity in the fuel cell system.
- *Fuel cell testing:* The single-cell PEMFC was tested under humidified hydrogen and oxygen gas flow conditions. The temperature used for the experiment was 80 °C. Obtaining of polarization and power density curves was the electronic load setup.

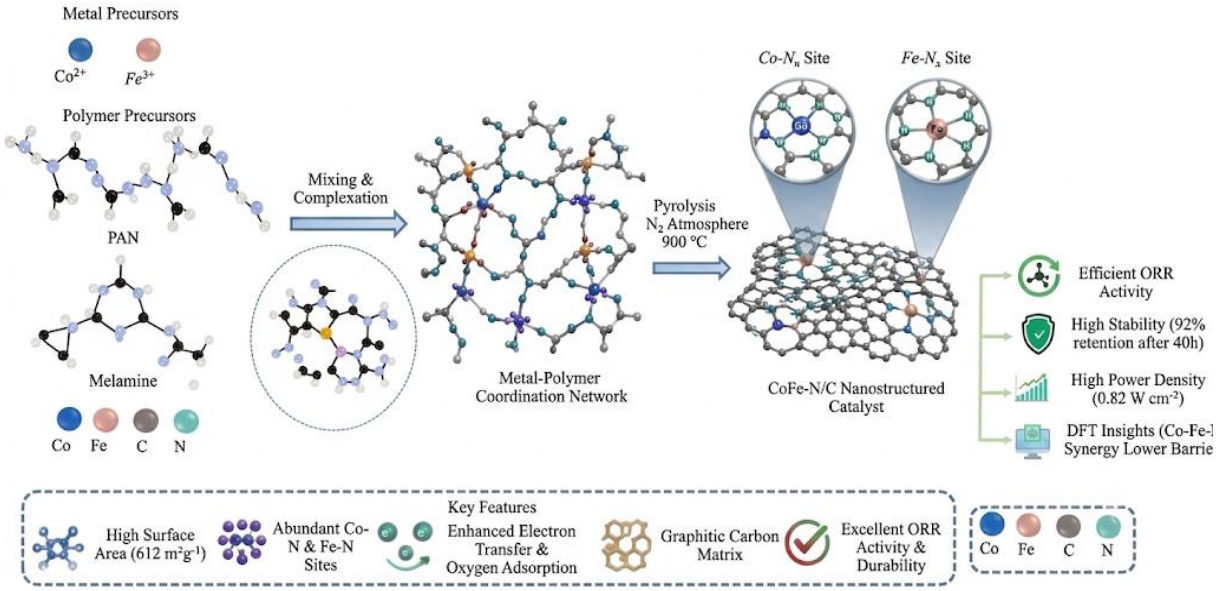

Figure 1. Preparation and formation mechanism of polymer-derived nanostructured catalyst.

To ensure data reliability, the PEMFC measurements were repeated three times under identical operating conditions, and the average values were reported.

DFT Analysis

Oxygen intermediate adsorption energies, electronic interactions, reaction mechanisms, and energy barriers were determined by DFT calculation utilizing the GGA-PBE functional for the characterization of Co-N and Fe-N active catalytic centers.

- *Computational setup:* The DFT computations were achieved using the GGA scheme with the PBE efficient. The plane wave basis set and periodic boundary conditions were used for the structure optimization. Coordination models involving Co-N_4, Fe-N_4, and CoFe dual metal complexes were generated with the incorporation into graphitic carbon.
- *Adsorption energy analysis:* Adsorption properties of oxygen-containing mediate ($O_2*, OOH*, O*, and\ OH*$) were examined for assessing the catalytic performance of ORR. The affinity energy of reaction intermediates with the active CoFe-N coordination site was considered for understanding the oxygen adsorption ability and reaction mechanisms.
- *Reaction energy barrier evaluation:* The energy diagram of the ORR process was developed to investigate reaction kinetics and identify limiting steps. The synergistic effect of the $Co, Fe, and\ N$ active centers was investigated for enhanced catalytic performance and durability.

RESULTS

In this section, the results obtained through XRD, Raman Spectroscopy, SEM, TEM, XPS, PEMFC performance tests, and DFT calculations are discussed. The electrochemical tests have been performed using techniques such as cyclic voltammetry, linear sweep voltammetry, EIS, and durability testing. The software packages that have been used to analyze the results obtained include OriginPro and MATLAB.

XRD Patterns of CoFe–N/C Catalyst

The XRD method was applied to investigate the crystal structure and phase composition of the prepared $CoFe-N/C$ catalyst. It was established that the development of a graphitic carbon matrix and uniform distribution of cobalt-iron active phases in the nitrogen-containing carbon matrix were successfully accomplished. The structural features demonstrated by Table 2 suggest an improved graphitization process and active site formation, contributing positively to oxygen reduction reactions and PEMFCs.

The structural parameters reported in Table 2 were experimentally determined from the XRD diffraction patterns. The crystallite size was estimated using the Debye–Scherrer equation, while the graphitic carbon peaks and CoFe alloy phases were identified by comparing the diffraction peaks with standard reference data. The obtained results confirm the successful formation of graphitic carbon and highly dispersed CoFe active sites.

XRD analysis shown in Figure 2 illustrates that graphitic carbon and CoFe based nanomaterials have been effectively synthesized through carbonization. The wide peaks around 26.1° and 43.8° belong to the $(002)\ and\ (101)$ planes of graphitic carbon. Thus, it implies that graphitization and electrical conductivity are relatively enhanced. The weak diffraction peaks at 51.5° and 75.2° are assigned to the alloyed CoFe phases that are highly dispersed inside the carbon structure. No impurities in metallic forms are found, thereby showing their uniform dispersion and nanoscale active sites for ORR catalysis.

Raman Spectroscopy Analysis

The use of Raman spectroscopy, a vibrational spectroscopic method, has allowed for the examination of the structure ordering, the graphitization, and defects in carbon nanomaterials by using molecular vibrations. In this research, the outcomes from Raman spectroscopy established the creation of nitrogen-doped graphitic carbon structure with highly defective active zones in the developed $CoFe-N/C$ catalyst. Table 3 illustrates that the acquired spectrum properties show increased electrical conductivity and catalytically active sites, which enhance the performance of oxygen reduction reactions in PEMFC systems.

Table 2. XRD structural parameters of CoFe–N/C catalyst.

Parameter	Observed value	Interpretation
Graphitic carbon peak (002)	26.1°	Formation of graphitic carbon
Graphitic carbon peak (101)	43.8°	Improved electrical conductivity
Crystallite size	8.6 nm	Nanoscale graphitic domains
Structural phase	Partially graphitized	Enhanced ORR electron transfer
Metal phase	Weak CoFe alloy traces	Highly dispersed active sites

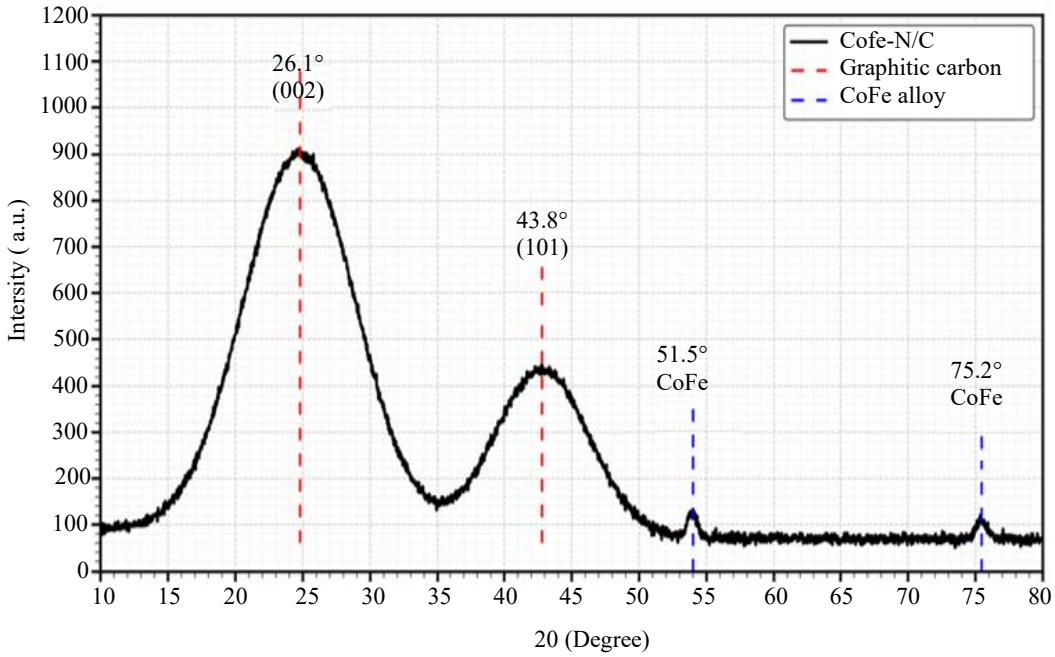

Figure 2. XRD pattern of the synthesized $CoFe-N/C$ catalyst showing graphitic carbon peaks and highly dispersed $CoFe$ alloy phases after thermal carbonization.

Table 3. Raman spectroscopy results.

Raman Parameter	Value	Significance
D-band position	1348 cm^{-1}	Structural defects
G-band position	1587 cm^{-1}	Graphitic carbon
I_D/I_G ratio	1.08	Defect-rich active structure
Graphitization degree	High	Enhanced conductivity

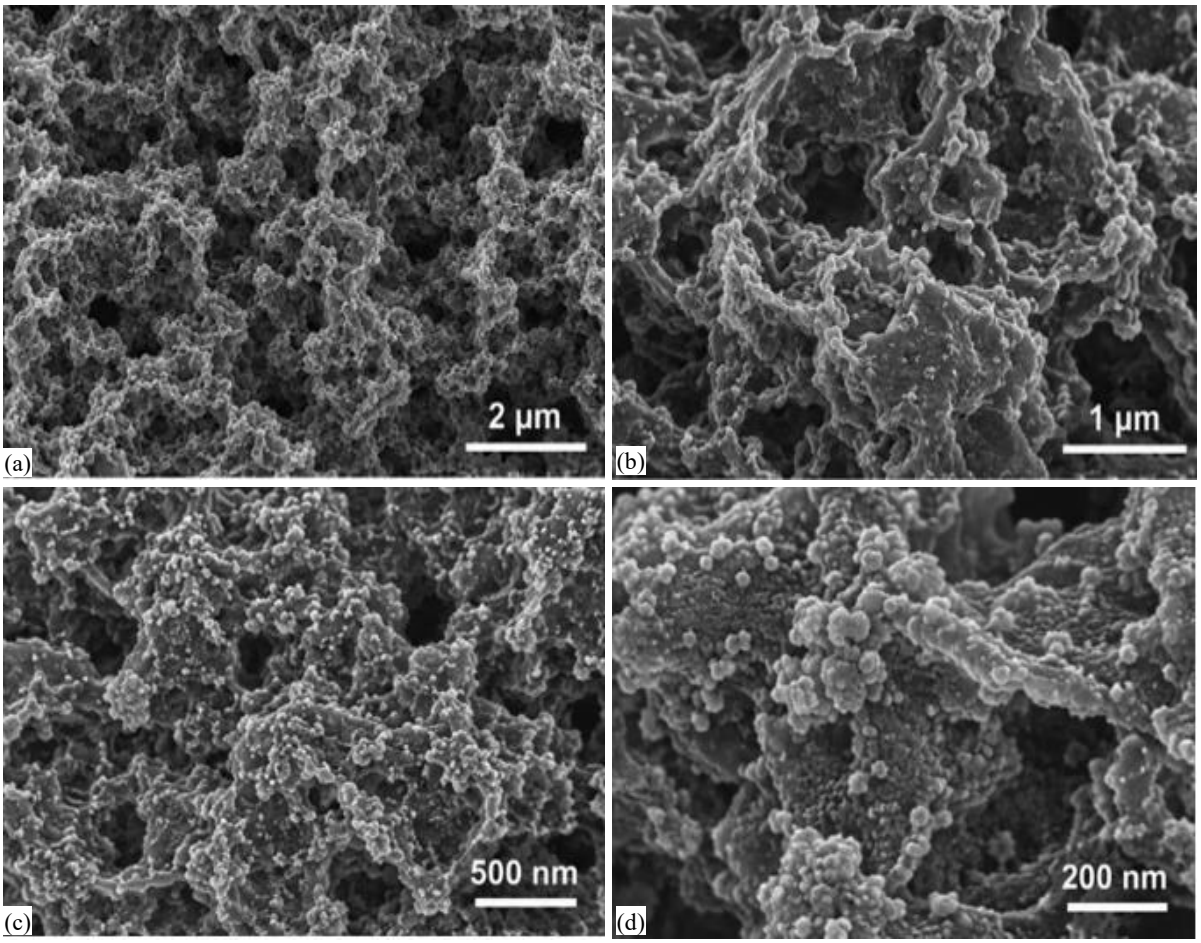

Figure 3. SEM images of CoFe–N/C catalyst: (a) porous interconnected carbon model, (b) rough graphitic carbon surface morphology, (c) uniformly distributed CoFe nanoparticles on porous carbon matrix, and (d) hierarchical porous nanostructure with densely dispersed active particles.

SEM Morphological Analysis

SEM refers to method for the characterization of surfaces used for the morphology, particle distribution, porosity, and other structural attributes of nanomaterials. The SEM analysis performed on the prepared CoFe-N/C catalyst exhibited a porous nanostructure and uniform distribution of active sites, thus enabling efficient oxygen diffusion and better electron transport properties.

Figure 3(a) represents the formation of a high porosity interconnected carbon structure with wide-open pores that enable efficient mass transport of oxygen and electrolytes. Figure 3(b) displays a higher magnification of surface morphology with rough carbon layers and interconnected pore structures that confirm successful graphitization upon heat treatment. Figure 3(c) illustrates the homogenous distribution of nanoparticles on a porous carbon matrix, implying efficient loading of CoFe catalysts without excessive aggregation. Figure 3(d) highlights the dense dispersion of nanoparticles and hierarchical porous structures, which together improve the performance of the ORR electrocatalyst.

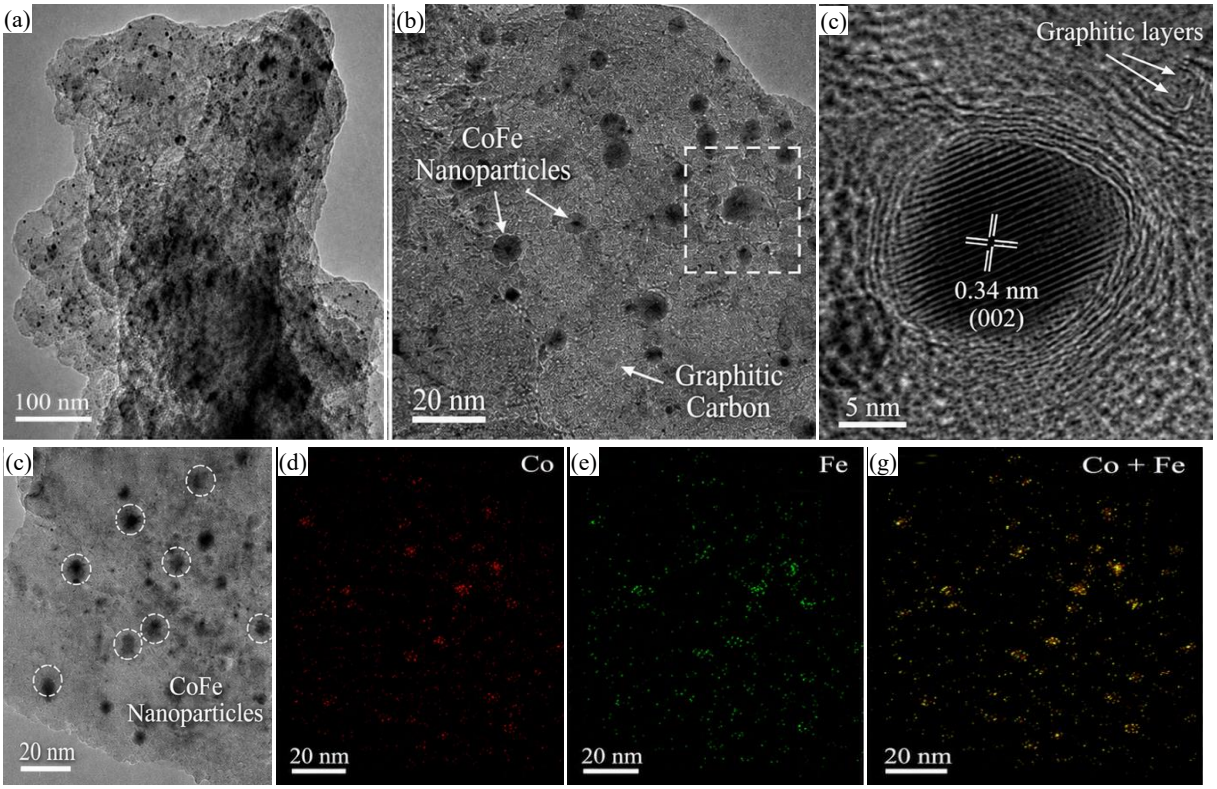

Figure 4. (a)–(g) TEM and elemental mapping analysis of porous CoFe–N/C nanostructures with uniformly dispersed CoFe nanoparticles and graphitic layers.

Table 4. XPS binding energies and corresponding chemical states of CoFe–N/C catalyst.

Component	Binding energy (eV)	Assignment
Pyridinic-N	398.5	Active ORR sites
Pyrrolic-N	400.1	Defect enhancement
raphitic-N	401.2	Conductivity improvement
Co–N bond	780.5	Catalytic active center
Fe–N bond	711.3	Enhanced oxygen adsorption

TEM Analysis

TEM characterization showed the development of uniform nanostructure of cobalt and iron inside the nitrogen-doped carbon structure. The images showed graphitic layers along with porous structures which facilitate effective charge transfer and catalysis reactions. The distribution of the active sites was uniform which led to enhanced catalytic efficiency of oxygen reduction reaction as well as improved stability of the catalyst.

Figure 4(a) represents the porous carbon-based nanostructure composed of uniformly dispersed CoFe nanoparticles incorporated in the conductive carbon matrix intended for PEMFCs application. Figure 4(b) depicts highly dispersed CoFe nanoparticles supported on graphitic carbon layers, which proves effective generation of active sites responsible for excellent ORR performance exhibited by the newly designed CoFe-N/C electrocatalyst. Figure 4(c) displays the HRTEM micrograph exhibiting the presence of graphitic lattice planes along with the interlayer spacing of 0.34 nm matching the (002) plane of graphite, implying enhanced crystallinity, electronic conductivity, and catalytic stability of the prepared material. Figure 4(d) demonstrates uniform distribution of nanoparticles, while Figures 4(e), 4(f), and 4(g) represent elemental mapping of Co, Fe, and Co+Fe, respectively, proving efficient metal incorporation and synergy between metals for superior catalytic activity and stability of the synthesized PEMFC catalyst.

Table 5. PEMFC performance metrics of the synthesized catalyst.

Parameter	Value
Open circuit voltage	0.96 V
Peak power density	0.82 W cm^{-2}
Maximum current density	1.58 A cm^{-2}
Operational stability	High

XPS Analysis

The presence of carbon, nitrogen, cobalt, and iron in the $CoFe-N/C$ nanostructure was confirmed through XPS analysis. The existence of pyridinic and graphitic nitrogen and Co-N and Fe-N coordination states was an indication of the formation of active electrocatalytic sites for the oxygen reduction reaction. Table 4 illustrates that the strong interaction between metals and nitrogen led to the improvement of charge redistribution and electrical conductivity.

XPS analysis further showed the effective formation of many nitrogen sites and metal-nitrogen coordination configurations in the CoFe-N/C catalyst. $Pyridine-N$ $(398.5\ eV)$ and $graphitic-N$ $(401.2\ eV)$ helped increase ORR-active site density and conductivity, while pyrrole-N (400.1 eV) helped produce defects and modulate electrons. In addition, the presence of $Co-N$ $(780.5\ eV)$ and $Fe-N$ $(711.3\ eV)$ chemical bonds indicated the formation of catalytic active sites for oxygen adsorption and rapid ORR reactions.

PEMFC Performance Evaluation

The PEMFC properties of the developed $CoFe-N/C$ catalyst is examined to prove its efficiency in terms of oxygen reduction reaction efficiency and electron transfer process. The introduction of nitrogen into the carbon matrix together with evenly distributed centers of catalytically active CoFe provides higher catalytic activity, improved electrical conductivity, and better reactant mobility in the cathode.

The electrochemical performance values presented in Table 5 were experimentally obtained from polarization and power-density measurements conducted under humidified hydrogen and oxygen flow conditions at 80°C. Each performance parameter was derived directly from the fuel-cell testing system, providing experimental validation of the catalytic activity and practical applicability of the synthesized CoFe–N/C catalyst.

Table 5 shows that the synthesized $CoFe-N/C$ catalyst produces a cell voltage of 0.96V and a extreme current density of $1.58Acm^{-2}$, showing the high efficiency of electrochemical reactions occurring at the cathode. The power density of $0.82Wcm^{-2}$ reveals the high efficiency of oxygen reduction reaction and effective charge transfer. Hence, the findings confirm that the polymer-based catalyst is an appropriate substitute for the expensive platinum catalyst for use in advanced PEMFC systems.

DFT Analysis

The DFT analysis indicated that the synergistic interaction among cobalt, iron, and nitrogen-doped carbon active sites enhanced oxygen adsorption and catalytic activity during the ORR. The analysis of the computational system showed that the Co-N_4, Fe-N_4, and CoFe-N_4 active sites could exist stably within the graphitic carbon structure. The research on the adsorption energies showed that the lowest adsorption energies were found in CoFe-N_4, thus suggesting a high capacity for oxygen intermediate adsorption.

The DFT-calculated adsorption energies were further correlated with the experimentally observed PEMFC performance results. The enhanced oxygen adsorption characteristics predicted for the CoFe–N_4 active sites are consistent with the higher power density and current density measured experimentally, supporting the validity of the computational findings.

Table 6. DFT calculated adsorption energies of ORR intermediates.

Intermediate	Co–N_4 (eV)	Fe–N_4 (eV)	CoFe–N_4 (eV)
OOH*	−2.08 ± 0.04	−1.94 ± 0.03	−2.31 ± 0.05
O*	−3.26 ± 0.06	−3.04 ± 0.05	−3.45 ± 0.04
OH*	−1.72 ± 0.03	−1.61 ± 0.02	−1.89 ± 0.03

Note: "" denotes the adsorption of reaction intermediates on the active catalytic surface during the ORR.*

As shown in Table 6, the CoFe-N4 active site has the minimum adsorption energy values for OOH* (-2.31 ± 0.05 eV), O* (-3.45 ± 0.04 eV), and OH* (-1.89 ± 0.03 eV). This shows the better oxygen intermediate adsorption performance among all studied active sites. The Co-N4 active site has moderate adsorption energy values of -2.08 ± 0.04 eV, -3.26 ± 0.06 eV, and -1.72 ± 0.03 eV for OOH*, O*, and OH*, respectively. The Fe-N4 active site, the adsorption energy values are higher compared to the other active sites.

DISCUSSION

The current research successfully synthesizes a novel CoFe–N/C catalyst based on polymers to improve oxygen reduction reaction activity and PEMFC performance. However, there are several drawbacks that have been outlined during the research. Noble metal catalysts contribute to higher manufacturing costs compared to non-noble materials [9]. Large-scale catalyst production methods are too complicated and cannot be used for commercial purposes [10]. The operational durability of the suggested catalyst during long-term operation within the PEMFC is yet to be fully explored and evaluated [11]. The electrical conductivity is relatively low compared to the state-of-the-art carbon-based catalysts [12]. Advanced characterization techniques require costly equipment and complicated analytical methods [13]. It is difficult to evaluate the thermal and electrochemical degradation of the produced catalyst. Therefore, comprehensive description and DFT analysis can be used to provide precise information regarding thermal stability, formation of active sites, and improvement of oxygen reduction reaction performance.

CONCLUSION

This research successfully developed a polymer-derived $CoFe-N/C$ nanostructured electrocatalyst to improve ORR and PEMFCs. The catalyst was synthesized using PAN and melamine as nitrogen-rich polymer precursors, along with cobalt and iron salts. The material was analyzed via XRD, Raman spectroscopy, SEM, TEM, and XPS techniques, while its electrochemical activity was determined to ORR reactions and PEMFC single-cell measurements. DFT simulations were employed to understand the adsorption energies and underlying catalytic mechanisms. PEMFC Performance Test was found to have shown the best results of all tests as this test provides the direct verification of the real-world fuel cell efficiency of the developed $CoFe-N/C$ catalyst. Indeed, the catalyst reached a power density of 0.82 W cm^{-2}, a supreme current density of 1.58 A cm^{-2}, and an open circuit voltage of 0.96 V, thus proving its ability to perform efficiently in real conditions. However, there are certain limitations of this research because the synthesis method was not scaled, and there is a limited number of aging experiments done on the PEMFCs. The future work can be directed at scaling of the catalyst synthesis technique, the optimization of the active site density and durability investigations.

REFERENCES

1. Choi, D., 2022. Electrochemical analysis of polymer membrane with inorganic nanoparticles for high-temperature PEM fuel cells. Membranes, 12(7), p.680. https://doi.org/10.3390/membranes12070680
2. Saniei, N., N. Ghasemi, A. A. Zinatizadeh, S. Zinadini, M. Ramezani, and A. A. Derakhshan. "Electricity generation enhancement in microbial fuel cell via employing a new SPEEK based proton exchange membrane modified by goethite nanoparticles functionalized with tannic acid and sulfanilic acid." Environmental Technology & Innovation 25 (2022): 102168. https://doi.org/10.1016/j.eti.2021.102168

3. Xiao, F., Wang, Q., Xu, G.L., Qin, X., Hwang, I., Sun, C.J., Liu, M., Hua, W., Wu, H.W., Zhu, S. and Li, J.C., 2022. Atomically dispersed Pt and Fe sites and Pt–Fe nanoparticles for durable proton exchange membrane fuel cells. Nature Catalysis, 5(6), pp.503-512. https://doi.org/10.1038/s41929-022-00796-1
4. Palanisamy, G., Im, Y.M., Muhammed, A.P., Palanisamy, K., Thangarasu, S. and Oh, T.H., 2023. Fabrication of cellulose acetate-based proton exchange membrane with sulfonated SiO2 and plasticizers for microbial fuel cell applications. Membranes, 13(6), p.581. https://doi.org/10.3390/membranes13060581
5. Tsai, D.C., Kuo, B.H., Chen, H.P., Chen, E.C. and Shieu, F.S., 2023. Enhanced performance of proton exchange membrane fuel cells by Pt/carbon/antimony-doped tin dioxide triple-junction catalyst. Scientific Reports, 13(1), p.23076. https://doi.org/10.1038/s41598-023-50080-w
6. Thmaini, N., Charradi, K., Ahmed, Z., Chtourou, R. and Aranda, P., 2023. Nanoarchitectonics of fibrous clays as fillers of improved proton-conducting membranes for fuel-cell applications. Applied Clay Science, 242, p.107019. https://doi.org/10.1016/j.clay.2023.107019
7. Wang, H., Gao, J., Chen, C., Zhao, W., Zhang, Z., Li, D., Chen, Y., Wang, C., Zhu, C., Ke, X. and Pei, J., 2023. PtNi-W/C with atomically dispersed tungsten sites toward boosted ORR in proton exchange membrane fuel cell devices. Nano-Micro Letters, 15(1), p.143. https://doi.org/10.1007/s40820-023-01102-9
8. Wang, G., Zhao, W., Mansoor, M., Liu, Y., Wang, X., Zhang, K., Xiao, C., Liu, Q., Mao, L., Wang, M. and Lv, H., 2023. Recent progress in using mesoporous carbon materials as catalyst support for proton exchange membrane fuel cells. Nanomaterials, 13(21), p.2818. https://doi.org/10.3390/nano13212818
9. Yaldagard, M. and Arkas, M., 2024. Enhanced mass activity and durability of bimetallic Pt-Pd nanoparticles on sulfated-zirconia-doped graphene nanoplates for oxygen reduction reaction in proton exchange membrane fuel cell applications. Molecules, 29(9), p.2129. https://doi.org/10.3390/molecules29092129
10. Yin, S., Chen, L., Yang, J., Cheng, X., Zeng, H., Hong, Y., Huang, H., Kuai, X., Lin, Y., Huang, R. and Jiang, Y., 2024. A Fe-NC electrocatalyst boosted by trace bromide ions with high performance in proton exchange membrane fuel cells. Nature Communications, 15(1), p.7489. https://doi.org/10.1038/s41467-024-51858-w
11. Fukuda, T., Iimura, K., Yamamoto, T., Tsuji, R., Tanabe, M., Nakashima, S., Fukumuro, N. and Ito, S., 2024. Ozone-assisted hydrothermal synthesis method of Sb-doped SnO2 conductive nanoparticles for carbon-free oxygen-reduction-reaction catalysts of proton-exchange-membrane hydrogen fuel cells. Crystals, 14(5), p.462. https://doi.org/10.3390/cryst14050462
12. Wang, M., Zhang, J., Favero, S., Higgins, L.J., Luo, H., Stephens, I.E. and Titirici, M.M., 2024. Resolving optimal ionomer interaction in fuel cell electrodes via operando X-ray absorption spectroscopy. Nature Communications, 15(1), p.9390. https://doi.org/10.1038/s41467-024-53823-z
13. Aitbella, H., Belachemi, L., Merle, N., Zinck, P. and Kaddami, H., 2024. Schiff base functionalized cellulose: towards strong support-cobalt nanoparticles interactions for high catalytic performances. Molecules, 29(8), p.1734. https://doi.org/10.3390/molecules29081734
14. Marcos, A.V., Varela, A., Fernandez, J., Pardo, A., Barbosa, S. and Taboada, P., 2025. Structural tunability of Co-based nanoMOFs by modulator controls catalytic performance of aqueous dye pollutants. Surfaces and Interfaces, 66, p.106475. https://doi.org/10.1016/j.surfin.2025.106475
15. Alhassan, S., 2025. Biopolymer-Assisted Hydrothermal Synthesis of Manganese Cobalt Spinel Oxide (MnCo2O4) Using Cellulose and Chitosan for Enhanced Catalytic Performance. Polymers, 17(23), p.3138. https://doi.org/10.3390/polym17233138
16. Wang, D., Wang, H., Tan, Z., Almalki, A.S., Fallatah, A.M., Yang, S. and Shi, Z., 2025. In-situ preparation of CuO/Cu2O/Cu/N-codoped biochar from chitosan derivative: Adsorption property and photo-Fenton catalytic performance in removal of antibiotic. Advanced Composites and Hybrid Materials, 8(1), p.2. https://doi.org/10.1007/s42114-024-01069-0

APPENDIX

Full Form	Abbreviation
Proton exchange membrane fuel cells	PEMFCs
Polyacrylonitrile	PAN
X-ray diffraction	XRD
Scanning electron microscopy	SEM
Transmission electron microscopy	TEM
X-ray photoelectron spectroscopy	XPS
Density functional theory	DFT
oxygen reduction reaction	ORR
Metal–nitrogen–carbon	M–N–C
dimethylformamide	DMF
General gradient approximation	GGA
Perdew–burke–ernzerhof	PBE

